phys. stat. sol. (c) **2**, No. 1, 294–297 (2005) / **DOI** 10.1002/pssc.200460168

Evidence for a universal relationship between magnetization and changes in the local structure in $La_{1-x}Ca_xMnO_3$

Frank Bridges[*1], **Lisa Downward**[1], **Shawna Bushart**[1], and **J. J. Neumeier**[2]

[1] Physics Dept. UCSC Santa Cruz, CA 95064, USA

[2] Physics Dept., Montana State University, Bozeman, MT 59717-3840, USA

Received 11 July 2004, revised 29 August 2004, accepted 17 September 2004
Published online 20 January 2005

PACS 61.10.Ht, 71.23.–k, 71.27.+a, 72.15.Qm

Ca dopants introduce holes in the Mn e_g band which allows electronic transport; such samples exhibit a colossal magnetoresistance (CMR) when the sample becomes ferromagnetic at low T, for x in the range 0.2 $<$ x $<$ 0.5. Previous EXAFS studies on the perovskite manganites $La_{1-x}Ca_xMnO_3$ indicated a correlation between changes in the local structure associated with polaron formation, and the sample magnetization for these samples. We have extended the EXAFS measurements to a wider range of Ca concentrations and to very high magnetic fields. Applying a magnetic field reduces the local distortion of each sample for temperatures near T_c. These measurements provide clear evidence for a universal relationship between the local structure and the sample magnetization. For at least one sample (x = 0.3), there is still a significant change of σ^2 with T below T_c when the sample is fully magnetized, i.e. distortions are still present and continuing to be removed as T is lowered well below T_c.

When $LaMnO_3$ is doped with Ca it introduces holes into the Mn e_g band which leads to novel transport and magnetic properties such as colossal magnetoresistance (CMR) and ferromagnetism, particularly for Ca concentrations in the range 20-50% [1]. At high T, the system is a paramagnetic insulator (semiconductor); in this regime, the electrical conductivity takes place via hoping polarons which produce a broadened distribution of Mn-O bond lengths. At low T, the system is a ferromagnetic metal; in this case the electrons become delocalized and most (in some cases all) of the local distortions disappear.

For $LaMnO_3$ there are four 3d electrons on each Mn atom (Mn^{+3}). Three are tightly bound (in a t_{2g} state) and form a spin 3/2 moment. The forth electron is in the half-metallic e_g band and is Hund-rule coupled parallel to the core Mn spin. Holes in this band (from doping with a divalent atom) provide the electrical transport (See Fig. 1). In the CMR regime, the ferromagnetic coupling is mediated through the double exchange interaction in which electrons (or holes) hop rapidly from one Mn atom to the next via an intervening O atom [2]. If the Mn spins are parallel, the electrons can hop rapidly with no spin flip; if the Mn spins are not parallel, it costs additional energy as the spin must also flip (See Fig. 1). As T approaches T_c, the hopping slows down – the lattice has time to partially respond and a Jahn-Teller distortion begins to appear (with two longer and four shorter Mn-O bonds). This enhances the metal to insulator transition [3].

Much work has been done on these systems - yet the way in which the magnetization develops is still not clear. Our earlier work [4, 5] shows that there is a connection between changes in the local distortion (which we associate with a decrease in the polaron distortion) and the magnetization as T is lowered through the ferromagnetic transition temperature T_c; the hopping increases as the spins become aligned and the distortion decreases. Although the concentration of holes is considerably less than 50%, all the Mn moments become aligned - except for samples close to the boundary between the ferromagnetic metal and the ferromagnetic insulator regimes, at roughly 18-20% Ca.

* Corresponding author: e-mail: bridges@frosty.ucsc.edu, Phone: +001-831-459-2893, Fax: +001-831-459-2893

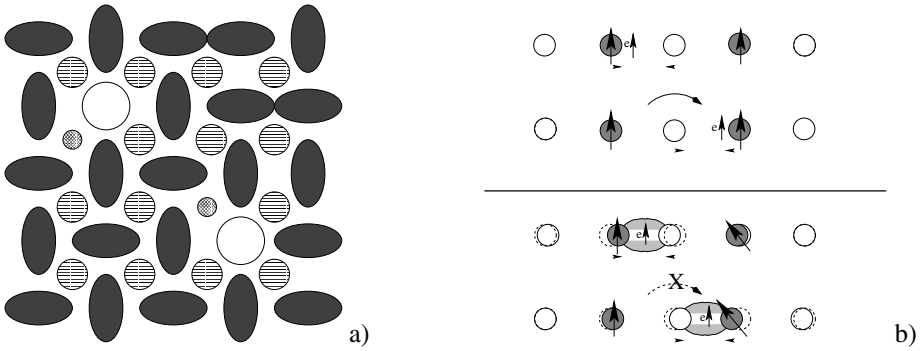

Fig. 1 a) A sketch of the holes on the Mn sites produced by Ca defects - black ovals, distorted Mn sites; open circles, (Mn) hole sites; horizontal stripes, La; small circle, Ca. The O atoms between the Mn are not shown and the La/Ca atoms are in layers above or below the Mn layer. b) A "cartoon" of the double exchange interaction - when moments aligned electrons hop rapidly, no distortions. When the moments are not aligned, hopping is slower; the lattice has time to respond and distorts.

There is a large U parameter in these systems [6] which makes it energetically unfavorable to have two e_g electrons on a given Mn site. Consequently $LaMnO_3$ is an insulator. Holes must be present before electrons can hop - and therefore before the double exchange interaction can become operative. Our EXAFS measurements show that relatively little distortion is removed as the sample becomes magnetized until the fraction of aligned Mn atoms is slightly larger than 2x - i.e. twice the number of holes. This leads to a model in which the magnetization develops via pairs of Mn atoms (a hole site and an electron site).

EXAFS data as a function of T and of magnetic field B, up to 11T, were collected on fine powder samples at SSRL using Si (111) and (220) double monochromators. The data were reduced using standard procedures and fit [4] using theoretical functions generated by FEFF6/FEFF7 [7].

In Fig. 2a, we show the first (Mn-O) peak in the Fourier transform (FT) of the EXAFS data (r-space) as a function of B for T $\sim$ T_c = 190K (21% Ca). As the field increases, the peak amplitude increases which indicates a field-induced decrease in the local distortions. From these data we can extract the average width of the Mn-O bond length distribution, σ (we need a single parameter to compare with the sample magnetization M). σ^2 is a measure of the mean square variation (the variance) of the Mn-O bond length throughout the sample; it is a measure of the local distortions, and is plotted as a function of T for various magnetic fields in Fig. 2b. σ^2 increases rapidly near T_c and then varies more slowly with T well above T_c. Note that the range of T, for which the main change in σ^2 occurs, extends to higher T as B increases. This follows the behavior of the sample magnetization with B - see Fig. 2c. Similar plots of σ^2(T) are

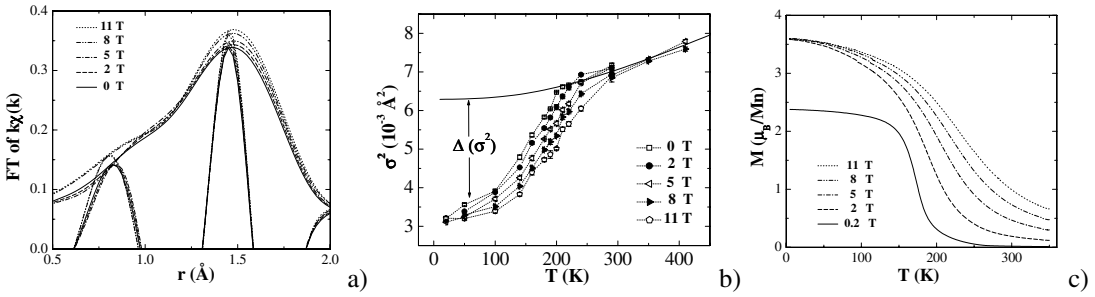

Fig. 2 21% Ca sample. a) Expanded view of the first (Mn-O) peak in the Fourier transform of the EXAFS data as a function of magnetic field near T_c; b) σ^2 as a function of T for several magnetic fields. c) shows the corresponding plots of $M(T)$ for the same applied fields.

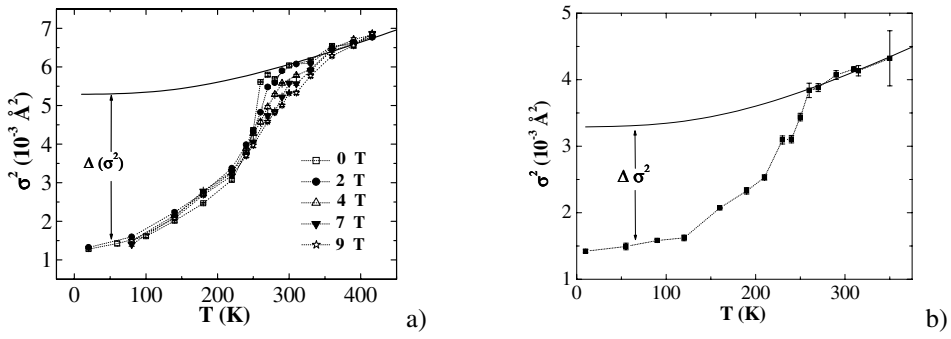

Fig. 3 a) Plot of σ^2(T) for Mn-O at various magnetic fields for 30% Ca. For this sample the magnetization is saturated at 150K, yet there is still a distortion of the Mn-O bond. b) A similar plot for the 45% Ca sample at B = 0T.

shown for the 30 and 45% samples in Fig. 3 and exhibit the same type of behavior; for the latter we only have data at B=0. For the 30% sample it is also clear that there is still some distortion left when the sample becomes fully magnetized that can be removed by lowering the temperature further - thus the double exchange mechanism is operative even when some distortion is present.

For comparison with M, we want a measure of the distortion removed as M increases. The change in σ^2, $\Delta\sigma^2$ is defined [4] in Fig. 2, 3, where the solid line represents normal phonon processes plus a large quasi-static distortion (produced by the polarons at high T). $\Delta\sigma^2$ is the difference between this line and the data. When we plot $\Delta\sigma^2$ vs M/M_o, all the data at various temperatures and different magnetic fields collapse onto a universal curve for a given concentration, as shown in Fig. 4a,b for the 21 and 30% samples; for the 45% sample we have only B=0T data. The break points are approximately at M/M_o = 0.45-0.5, 0.65 and 0.9 for $2x$ = 0.42, 0.6, and 0.9. (The solid lines in Fig. 4a,b are fits to a model in which the distortion per site is allowed to vary - with the lowest distortion sites becoming magnetized first - this is discussed elsewhere [8]).

The important point - particularly for the lower concentration samples - is that little distortion is removed until the sample is roughly 50% magnetized; then a large distortion is removed as M/M_o increases to 1. For the double exchange to operate, there must be adjacent electron and hole sites so that the electron can begin to hop back and forth quickly. The electron site will initially be J-T distorted while the hole site is, to lowest order, undistorted. When the electron hops fast enough, the distortion disappears. Thus if the magnetization grows initially via pairs of Mn atoms (a hole and an electron site – see Fig 5a), the net distortion removed per magnetized site is half that of the J-T distorted electron site; however, once all the holes are used up the distortion removed per magnetized site must be the full J-T distortion and $\Delta\sigma^2$ should increase twice as quickly with M/M_o. If there is a distribution of Jahn-Teller distortions (depending on the

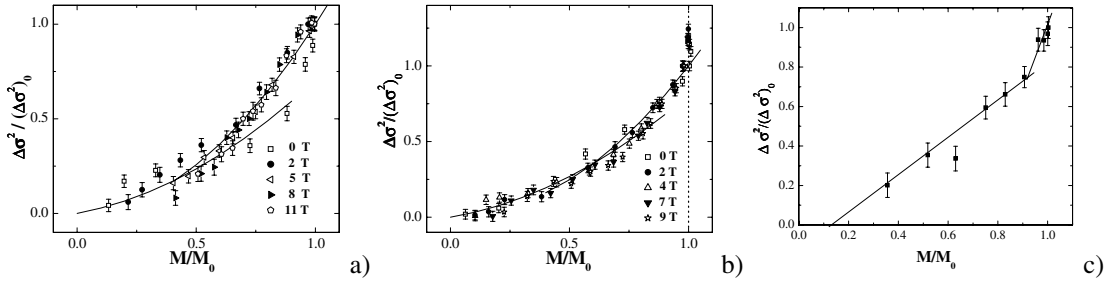

Fig. 4 $\Delta\sigma^2$ vs M/M_o for a) 21%, b) 30%, and c) 45% Ca. Solid lines are a fit to a model in which there is a range of J-T distortions (not discussed). Break points approximately at M/M_o = 0.45-0.5, 0.65, and 0.9, respectively.

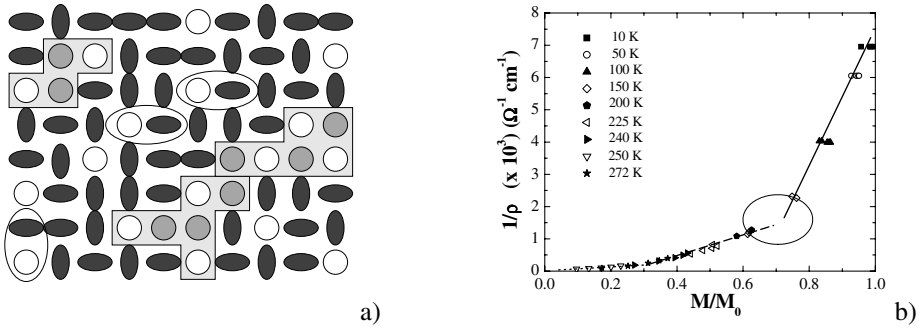

Fig. 5 a) Model of the magnetization process - Mn sites only. Black ovals, distorted Mn sites; open circles, hole sites; shaded regions, magnetized clusters. In the latter the electrons hop rapidly, the open circles show the original hole sites and the gray circles the original sites that became undistorted when the site became magnetized. b) Plot of the electrical conductivity ($\sigma_{el-cond}$ = 1/ρ) as a function of M/M_o for several temperatures from data of Hundley *et al* [9]. Multiple points at the same temperature are at different magnetic fields.

Ca distribution in the sample), then the smallest distortion (lowest strain energy) will become undistorted first.

To emphasize the interesting connections/couplings between the spin, the charge, and the lattice we replot some resistivity data for the 30% Ca sample [9] as the conductivity $\sigma_{el-cond}$ vs M/M_o in Fig. 5b ($\sigma_{el-cond}$ = 1/ρ). There is a clear break in $\sigma_{el-cond}$ at $M/M_o \sim 0.65$, in agreement with the EXAFS data. In addition there is also a break at $M/M_o \sim 0.3$ which is close to the percolation threshold!

Thus based on these results, the magnetization could develop as follows: at low M, small clusters form from adjacent pairs of hole and electron sites; as M grows (T decreases or B increases), unmagnetized hole sites diffuse close enough to a small magnetic cluster that another pair can join. This will lead to filamentary clusters of magnetic, conducting material. In this regime, the sample conductivity remains low. When the M/M_o reaches$\sim$ 0.31, 31% of the sites are magnetized and percolating clusters should form; then the conductivity will increase more rapidly as observed (Fig. 5b). As M/M_o increases further, the number of percolating filamentary clusters increases until all the hole sites are incorporated into the magnetic clusters. At this point, additional increases in M/M_o require that Jahn-Teller distorted sites between the filaments become magnetized - and conducting. This fills in the regions between the filaments, the Mn local distortions decrease significantly, and $\sigma_{el-cond}$ grows rapidly.

Acknowledgements The work at UCSC was supported in part by NSF grant DMR0301971. The experiments were performed at SSRL, which is operated by the DOE, Division of Chemical Sciences, and by the NIH, Biomedical Resource Technology Program, Division of Research Resources.

References

[1] P. Schiffer, A. Ramirez, W. Bao, and S-W. Cheong, Phys. Rev. Lett. **75**, 3336 (1995).
[2] C. Zener, Phys. Rev. **82**, 403 (1951); P. W. Anderson and H. Hasegawa, Phys. Rev. **100**, 675 (1955).
[3] A. J. Millis, B. I. Shraiman, and R. Mueller, Phys. Rev. Lett. **77**, 175 (1996); H. Röder, J. Zang, and A. R. Bishop, Phys. Rev. Lett. **76**, 1356 (1996).
[4] C. H. Booth, F. Bridges, G. H. Kwei, J. M. Lawrence, A. L. Cornelius, and J. J. Neumeier, Phys. Rev. Lett. **80**, 853 (1998); Phys. Rev. B **57**, 10440 (1998).
[5] D. Cao, F. Bridges, C. H. Booth, and J. J. Neumeier, Phys. Rev. B **62**, 8954 (2000).
[6] F. Bridges, C. H. Booth, G. H. Kwei, J. Neumeier, and G. A. Sawatzky, Phys. Rev. B **61**, R9237 (2000).
[7] S. I. Zabinsky, J. J. Rehr, A. Ankudinov, R. C. Albers, and M. J. Eller, Phys. Rev. B **52**, 2995 (1995).
[8] F. Bridges, L. Downward, S. Bushart, J. Neumeier, N. Dilley, and L. Zhou (unpublished).
[9] M. F. Hundley, M. Hawley, R. H. Heffner, Q. X. Jia, J. J. Neumeier, J. Tesmer, J. D. Thompson, and X. D. Wu, Appl. Phys. Lett. **67**, 860 (1995).